Journal of Structural Geology, Vol. 14, No. 2, pp. 181 to 192, 1992
Printed in Great Britain

0191-8141/92 $05.00+0.00

Evolution of stacked, ductile shear zones in carbonates from mid-crustal levels: Tuscan Nappe, N. Apennines, Italy

KAREN E. CARTER*

Department of Geological Sciences, University of Texas at Austin, Austin, TX 78713, U.S.A.

(*Received* 27 *November* 1990; *accepted in revised form* 21 *June* 1991)

Abstract—The evolution of ductile shear zones within the Portoro Limestone of the Tuscan Nappe, Portovenere region, Italy, has been determined using three-dimensional strain analysis. Shear zones, composed of calcite matrix and carbonate veins, are parallel to bedding and alternate with undeformed layers of mixed calcite and dolomite. The shear zones developed under conditions of non-coaxial, rotational deformation as determined from the rotation and shape change of veins within the shear zones and the angular relationship between the shear zone fabric and shear zone boundary. In addition, apparently complex flow that would be recorded by additional components of strain, such as layer-parallel shortening or extension or wrenching did not occur based on the lack of significant veins strike changes and pellet shape changes in sections parallel to the shear plane. Minor, localized volume loss occurred in some shear zones where high and low strains are juxtaposed. The shear zones, therefore, developed under conditions of non-coaxial rotational strain that was heterogeneously distributed along layers parallel to bedding and were locally accompanied by volume loss.

INTRODUCTION

SHEAR ZONES have enjoyed widespread interest in the past two decades at least in part because of their abundance throughout many orogenic belts (e.g. Carmignani *et al.* 1978, Berthé *et al.* 1979, Ramsay & Allison 1979, Ponce de Leon & Choukroune 1980, Ramsay 1980, Boullier 1986, Davis *et al.* 1986, Gapais *et al.* 1987, Ghosh & Sengupta 1987) and the diversity in their nature. Our understanding of shear zones, therefore, in terms of characteristics such as geometry, types of strain, microstructures, kinematic indicators and tectonic significance has increased dramatically. Only a fraction of this attention, however, has been devoted to the study of the evolution of ductile shear zones. Poirier (1980) suggests that shear zones initiate by localization on plastic instabilities, whereas Segall & Simpson (1986) have documented ductile shear zone nucleation on dilatant fractures that later experienced fluid-enhanced ductility. Once the shear zone has localized, Coward (1976) suggests that the propagation of ductile shear zones involves flattening strains at shear zone terminations so that the strain path can not be solely simple shear. Similarly, Ramsay & Allison (1979) propose that flattening strains exist at the terminations of ductile shear zones that die out into the host rock. If these types of strain accompany the nucleation and propagation of ductile shear zones they should be recorded within the zones as permanent deformation that can be quantified. In many cases, however, the shear zones do not contain information, such as passive markers or undeformed shear zone boundaries, that are needed for strain analysis or, alternatively, the strain record has been obscured by later deformation. As a result, natural examples of shear zones for which nucleation points and propagation paths have been determined are rare (Coward 1976).

In this paper I present the results from a study of closely-spaced, bedding-parallel ductile shear zones within the Portoro Limestone, Italy. The Portoro provides an unusual opportunity to study the evolution of ductile shear zones because it contains approximately 200 well-defined shear zones that are bounded by undeformed layers, contain a shear-related fabric and preserve abundant passive markers that also exist in adjacent undeformed layers. Additionally, the Portoro is extremely well exposed in large quarries so that sampling can provide excellent lateral and vertical control on the types and magnitudes of strain within individual shear zones.

GEOLOGIC SETTING

The Portoro Limestone is part of the La Spezia Formation (Ciarapica *et al.* 1985) of the Tuscan Nappe in the Portovenere area of the Northern Apennines (Fig. 1). The nappe presently forms a SW-vergent recumbent anticline that formed after Mid-Tertiary E-directed thrusting (Carter & Mosher 1987, Carter 1990, Carter *et al.* 1991). The units exposed within the nappe are the Tuscan continental shelf sequences that were studied in detail by Capellini (1862) and re-examined by Ciarapica *et al.* (1985). The oldest units in the core of the anticline, the La Spezia Formation and Calcari ad Angulati Formation (Table 1) were buried between 7 and 10 km, based on the thickness of overlying units (Fazzuoli 1980, Ciarapica *et al.* 1985). The Portoro Limestone is part of the La Spezia Formation and was deposited in the late Triassic as an aragonite mud that recrystallized to calcite microspar during shallow (<50°C) burial (Folk 1988). The unit is approximately 80 m thick and is composed of black calcite with alternating layers of mixed calcite and

*Present address: Department of Geology, Baylor University, Waco, TX 76798-7354, U.S.A.

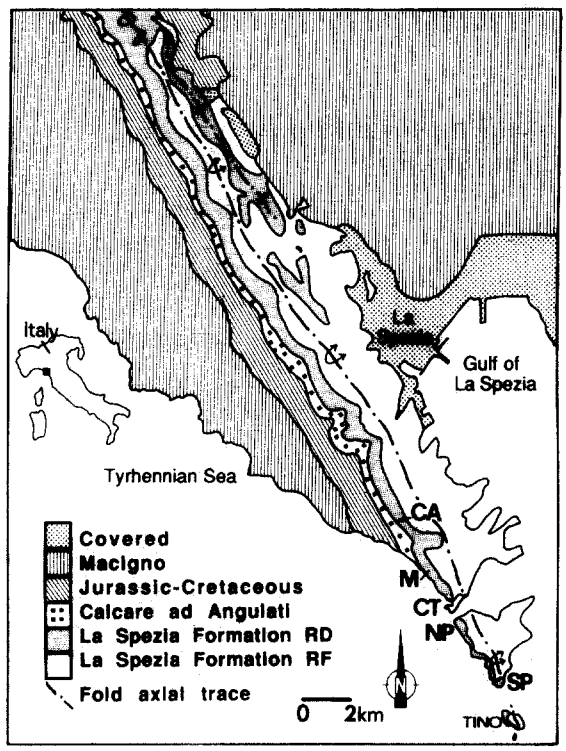

Fig. 1. Simplified geologic map of the La Spezia region after Zaccagna (1936). Units: La Spezia Formation RF—limestone with Avicula Contorta; La Spezia Formation RD—dolomite, limestone and calcareous breccia, contains Portoro Limestone; Jurassic through Cretaceous formations as listed in Table 1; MA—Macigno sandstone. Locations: SP—South Palmaria Island Quarry, NP—North Palmaria Island Quarry, CT—Cemetary Quarry, M—Muzzerone Quarry, CA—Monte Castellana.

dolomite. Bedding-parallel ductile shear zones have formed in the Portoro as a result of NE-directed Miocene thrusting that preceded folding (Carter & Mosher 1987, Carter 1990). The Portoro is found on the overturned limb and in the hinge regions of the fold; the best exposures are on the overturned limb. During shearing and low-grade metamorphism, fluid was channelized through the zones causing geochemical and petrographic changes (Carter 1990, Carter & Dworkin 1990). Later SW-vergent folding occurred at lower temperatures in the absence of fluids and was accomplished by slip along shaley layers and by the development of intense W-dipping mylonitic shear zones that cross-cut pre-existing bedding parallel shear zones (Carter 1990, Carter *et al.* 1991 and in preparation). Therefore, during folding, the Portoro, bounded by slip horizons, did not experience layer-parallel slip and behaved as a competent, massive block.

Shear zones in the Portoro Limestone

Extremely well exposed quarries of Portoro in the overturned limb of the anticline reveal a stack of more than 200 bedding-parallel ductile shear zones that alternate with undeformed layers on the scale of 10–20 cm (Figs. 2a–c). The undeformed layers contain mixed calcite microspar and dolomite. The calcite microspar forms an equant mosiac with a grain size of approximately 10–20 μm. Dolomite replaces calcite to varying degrees as a result of several episodes of dolomitization that began before lithification and continued intermittently into the Pleistocene (Miller 1988). In addition,

Table 1. Tuscan Nappe stratigraphy, La Spezia region

Epoch	Unit: Ciarapica *et al.* (1985)	Unit: Zaccagna (1936)	Lithology	Thickness* (m)
Oligocene	Macigno	ma	Sandstone, minor calcareous shale	>1500
Eocene–Late Cretaceous	Scisti Policromi	gl, sr	Marl	137
	Maiolica	ne	Limestone	17
Dogger–Malm	Diaspri	td	Chert, limestone	40
Lias	Marne e Posidonia	ls	Calcareous marl, marl	114
	Calcare selcifero	lm	Limestone	34
Early Jurassic	Rosso Ammonitico	tr	Limestone, shaley limestone	57
	Calcari ad Angulati	lg	Limestone, shaley limestone	142
Late Triassic	La Spezia Formation†	rd	Limestone, shaley limestone	200
	Strati di Coregna	rc	Dolomite	50

*Approximate.
†Contains Portoro Limestone.

Fig. 2. (a) Bedding-parallel shear zones alternate with undeformed layers in the Portoro Limestone. Deflection of veins in the shear zones shows east sense of shear (upper part moved toward the left). Abandoned quarry, south coast of Palmaria Island. View toward southeast, beds overturned. (b) Close up of shear zone outcrop at north Palmaria Island. Pretectonic veins form at high angles to bedding either at stylolites between sheared and unsheared layers, or cut through both types of layers. Deflection of veins and *S–C* morphology of grey nodules indicate east sense of shear (towards left). (c) Stacked, bedding-parallel shear zones in the central part of South Palmaria quarry. Bedding and shear zones (alternating light and dark layers) appear nearly horizontal. White areas are dolomitized. View west. (d)–(e) Photomicrographs of Portoro Limestone, southern Palmaria Island. (d) Microspar from undeformed layers shows an equant fabric with relatively straight grain boundaries. View parallel to strike of bedding. (e) Microspar from shear zones shows a grain shape fabric and wavy to sutured grain boundaries indicating dynamic recrystallization. View normal to *ac* plane. Bar scale is 0.5 mm.

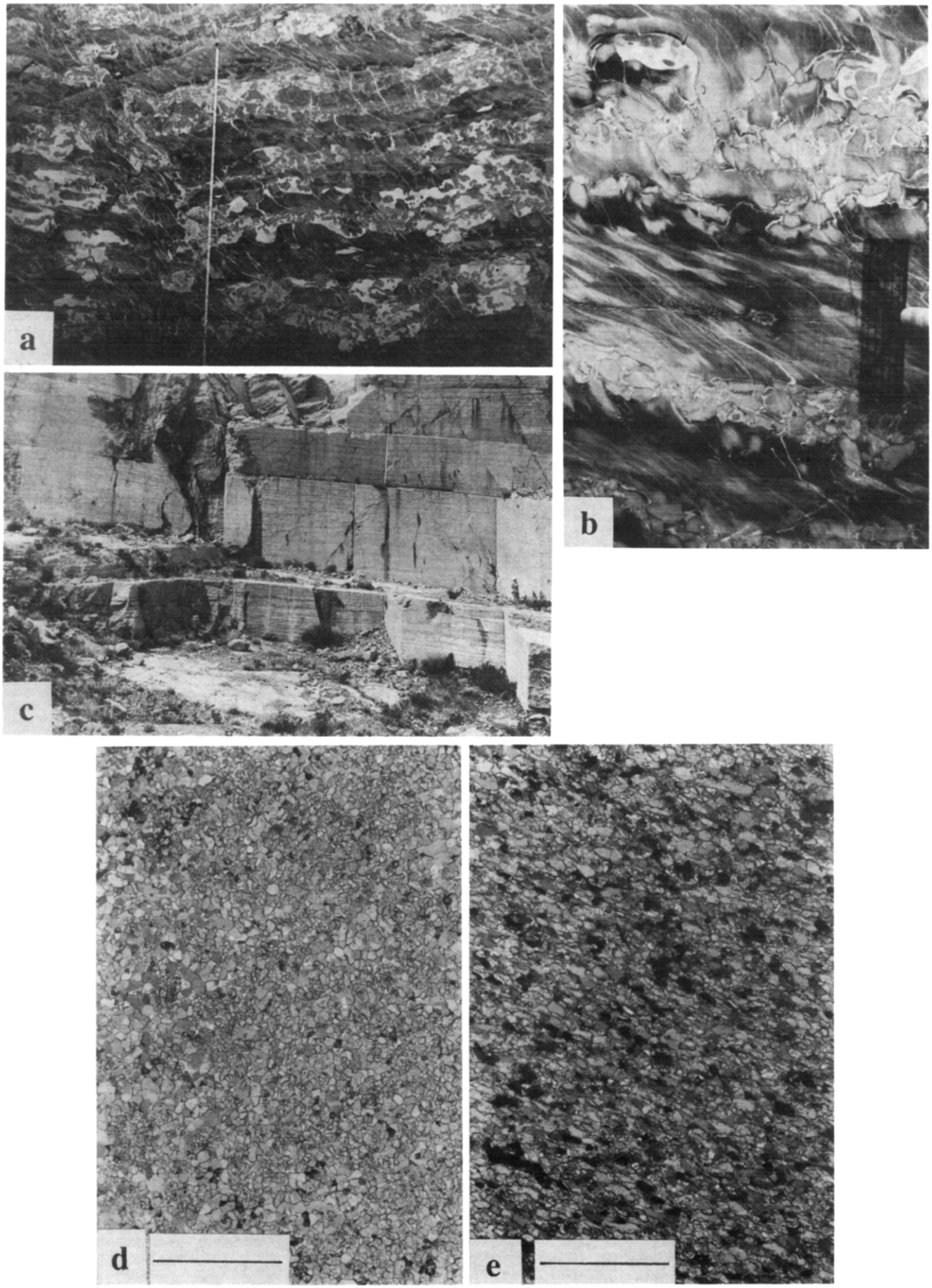

Fig. 2.

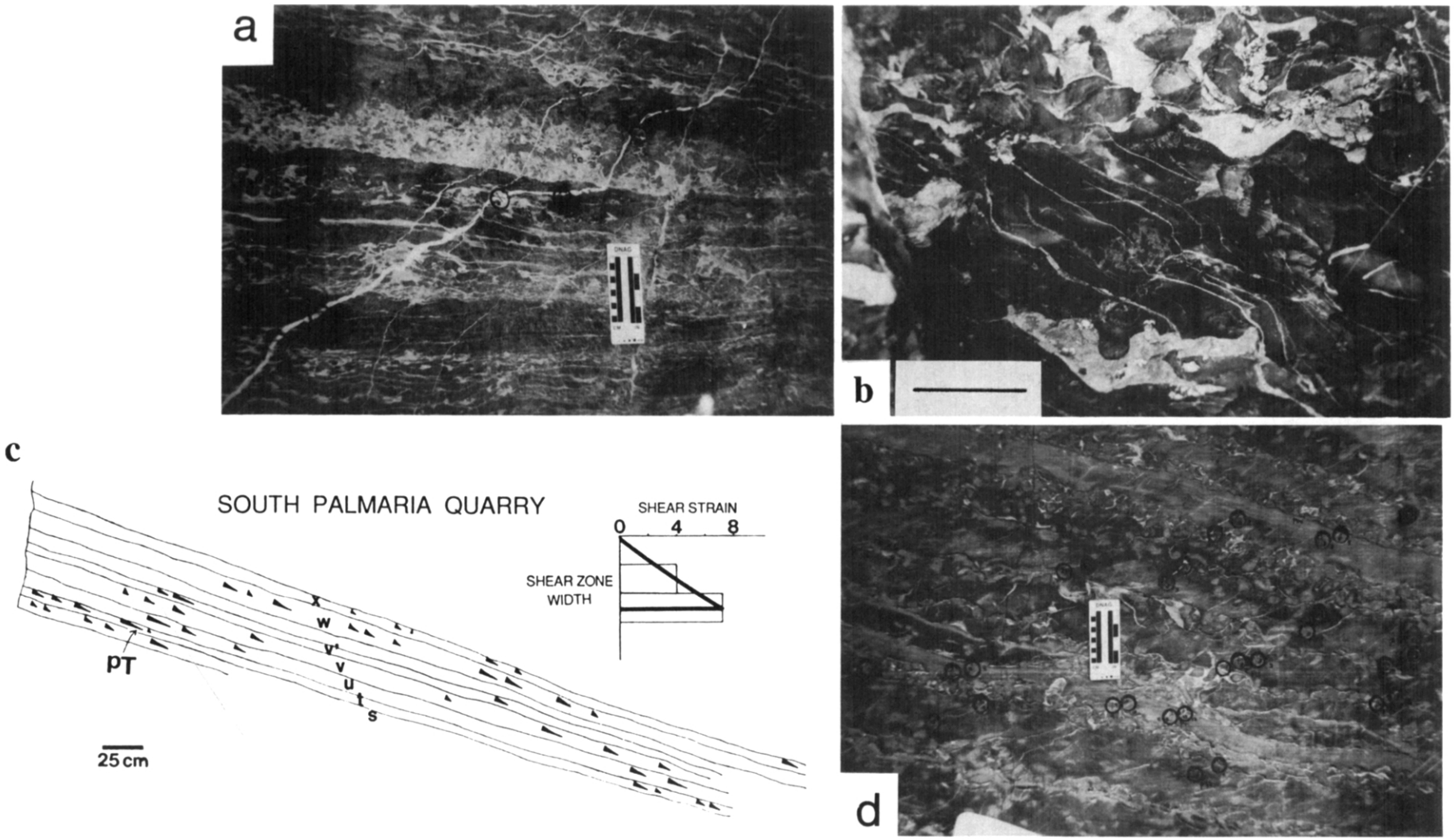

Fig. 6. (a) Quarry face at South Palmaria Quarry. Veins were sampled in undeformed and sheared layers. Photograph shows cored samples after drilling, prior to removal. View west. (b) Shear zone (horizontal) contains dolomitized regions and non-planar shear zone walls. Deflection of veins varies or changes in these areas as a result of perturbations to flow during deformation. Northern Palmaria Island, abandoned quarry. View south, bar scale is 8 cm. (c) Sketch of quarry face, core locations and shear strain magnitudes (see Fig. 9, upper right face). Note lateral variation in shear strain magnitudes. Zones labeled s–x. Adjacent large and small strain values likely indicate volume change, see for example pT. (d) Outcrop photograph of left side of shear zone shown in (c). Cores sampled at pT (immediately below scale toward the right) show change in shear strain from 1.78 to 0.15.

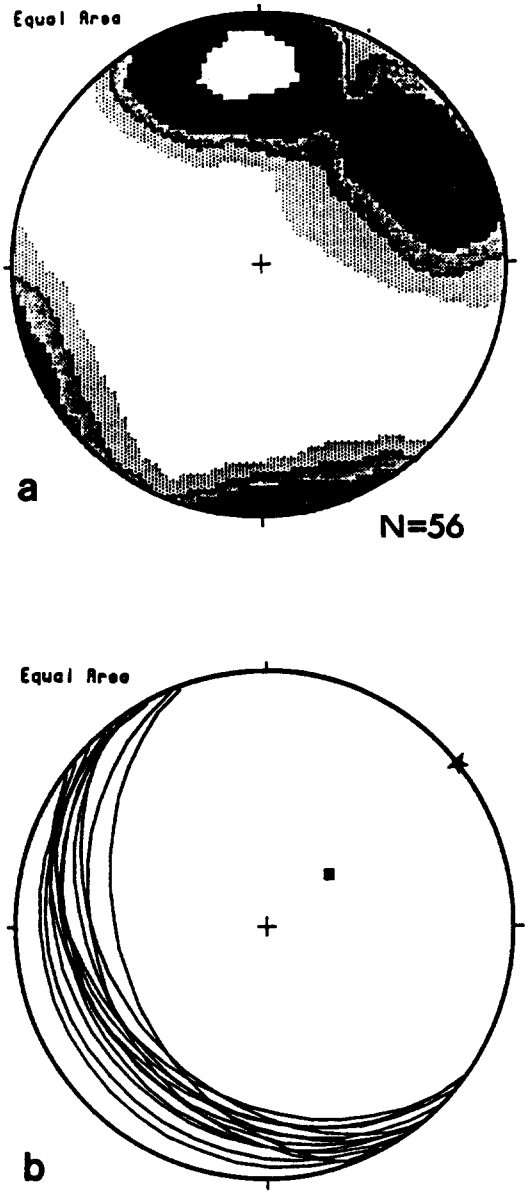

Fig. 3. Equal-area stereogram, lower-hemisphere projection; bedding rotated to original horizontal position. (a) Poles to veins in the undeformed layers show generally W- and NW-trending veins with steep dips. Contours 9, 7, 5, 3 and 1% per 1% area. (b) Average orientation of foliation surfaces in shear zones from each quarry shown by great circles. Square—pole to the average foliation surface; star—average direction of tectonic transport (*a*).

some undeformed layers contain crustacan fecal pellets that range in size from 0.1 to 1.5 mm. Nearly all undeformed layers are cut by coarse-grained calcite and dolomite veins that extend into shear zones. The veins are generally at a high angle to bedding and have many different orientations (Fig. 3a), colors and morphologies (see Folk *et al.* 1989). No grain shape fabrics are visible in these undeformed layers (see also Carter 1990) and grain boundaries are planar to slightly curved (Fig. 2d).

Shear zones are generally planar and separated from undeformed layers by stylolites that formed prior to shearing. The zones are composed of calcite microspar with a grain size between 10 and 20 μm. Dolomitization of the matrix is either non-existent or slight. As in undeformed layers, some shear zones contain fecal pellets. In addition, all shear zones contain the same pretectonic carbonate veins that are observed in underformed regions. These veins generally either cross-cut both undeformed layers and shear zones or extend from bedding-parallel stylolites within the undeformed layers into the adjacent sheared layer (Figs. 2a & b). The veins change orientations within the shear zones and usually form a smooth curved surface reflecting maximum shear strain in the center of the zones and progressively less shear strain approaching the shear zone boundaries. In highly strained zones, the veins become asymptotic with the shear zone. The veins record no evidence of prior or subsequent shearing in another direction. Calcite in most shear zones has a grain shape fabric with long axes at an acute angle to the shear zone boundary. Grain boundaries of the microspar are wavy and coarser grains in veins show twinning, serrated grain boundaries, and zones of very fine grains (Fig. 2e) (see also Carter 1990).

SHEAR ZONE GEOMETRY AND STRAIN

The multiple generations of pretectonic veins, shear-related foliation and pellets in the Portoro Limestone can be used to determine the type and amount of strain suffered in the shear zones. Nearly all veins formed at a high angle to bedding and range in strike from W to NNW (Fig. 3a). Most veins range in length from a few cm to tens of cm and stretch from undeformed layers into sheared zones (Figs. 2a & b). The most abundant veins are composed of 0.05–1 mm crystals of calcite with varying amounts of dolomite (see Folk *et al.* 1989). Because the veins have the same composition as the host matrix, they can be considered passive markers whose displacement in shear zones is a measure of strain (Ramsay 1967). If the orientation of these veins in their deformed and undeformed state is known, and the orientation of the foliation developed within the shear zone can be measured, the shear strain can be quantified according to the method developed by Skjernaa (1980). In simple shear deformation, all planar markers in a shear zone that are not parallel to the *ac* or shear (*ab*) plane will rotate about their strike toward parallelism with the shear plane (Fig. 4) with increasing

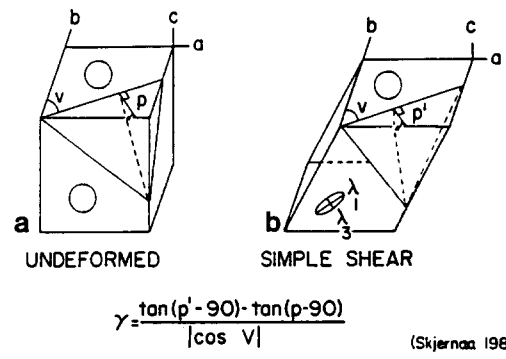

Fig. 4. Orientations of a pre-existing planar marker in the undeformed and deformed states. (a) Undeformed (circles), *v*—angle between *b*-direction and trace of marker on shear plane, *p*—angle between shear plane and planar marker. (b) Simple shear deformation, *p'*—new angle between shear plane and planar marker, *v* does not change. No strain occurs in shear plane (circle). Equation rearranged from Skjernaa (1980), appendix equation (2).

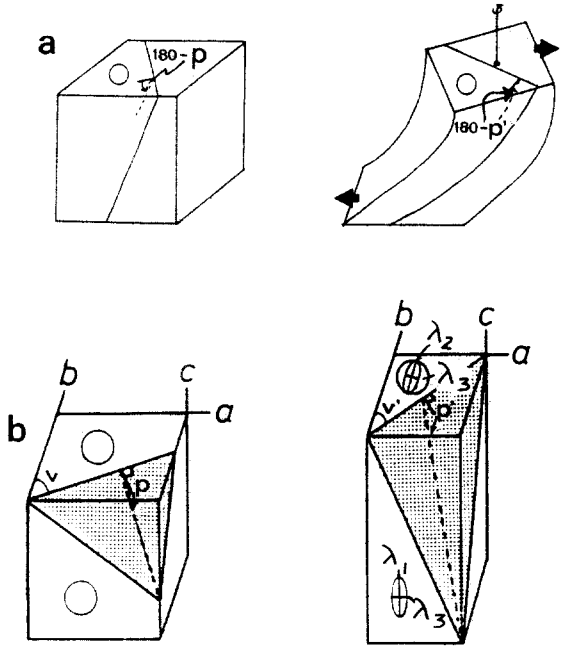

Fig. 5. (a) Wrench-type shear, rotation around a vertical axis during simple shear. p'—new angle between shear plane and planar marker. Strike of vein is different from strike in undeformed state. (b) Pure shear. p' as in (a); v'—new angle between b-direction and trace of plane on shear plane.

strain according to the following equation (Skjernaa 1980):

$$\gamma = [\tan(p' - 90) - \tan(p - 90)]/|\cos v|, \quad (1)$$

where p and p' are the angles between the veins and the shear plane in the undeformed and deformed states, respectively ($0 \leq p, p' < 180°$), and v is the angle between the strike of the vein on the shear plane and the b-direction ($0 \leq v < 180°$).

If the plane strain deformation within shear zones results from additional components of strain, it should be reflected by the orientations of the veins and possibly the foliation. Wrench-type shear (Sanderson 1982, i.e. rotation about c causing a displacement gradient in the ab plane), for example, would produce a unidirectional rotation of vein strikes (Fig. 5a). Longitudinal strain parallel to the shear plane would produce a change in the angle v (Fig. 5b) and p' as a function of the amount and orientation of strain and the orientation of the undeformed vein. The strain ratio resulting from shortening or extension along the shear plane can be determined with a Mohr construction described by Ramsay (1967, pp. 76–78). The effects of such longitudinal strain or volume change not parallel or perpendicular to the ab plane would also be recorded by the shape change of pellets in sections parallel to the shear plane and could be quantified by standard methods (Fry 1979) (see later discussion on strain results and interpretations).

Sample techniques and locations

Approximately 400 veins were selected for strain analysis from five Portoro quarries on the overturned limb of the La Spezia fold (Fig. 1). Three of the quarries

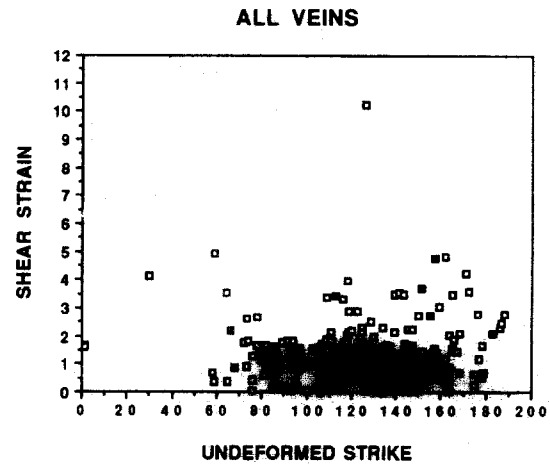

Fig. 7. Shear strain measured using change in dip angle vs trend of trace of same vein on plane parallel to shear zone boundary (vein strike) in undeformed layer. Filled squares represent dolomitic veins, unfilled represent calcite veins.

(M, CT and NP), expose the lower stratigraphic half of the Portoro. The mid section of the Portoro is exposed in the northernmost quarry (CA), and the entire Portoro section is visible at the southernmost, largest quarry (SP). Seven large samples of undeformed layers containing veins were taken from three locations, NP, SP and CT, for the purpose of determining the natural variation in strikes of individual veins within undeformed layers. From these samples, serial slabs were cut parallel to the shear plane and strikes were recorded for a total of 54 veins that were traced through slabs. At each of the five quarries, the foliation and the shear zone boundaries, which are parallel to bedding, were determined. In addition, because of the difficulty of measuring veins in three dimensions on planar, vertical quarry faces, veins in shear zones and in adjacent undeformed layers were cored with a drill-modified chainsaw. More than 700 cores were drilled through veins that were visibly deflected from undeformed into sheared layers (Fig. 6a) in five quarries. Using an adjustable apparatus, these cores were reoriented in the laboratory to their field position and the orientations of internal veins were measured. The original orientation of veins and foliations were obtained by rotating bedding, which is parallel to shear zone boundaries, about the major fold axis to its original horizontal position.

Strain results and interpretations

Shear strains. Pretectonic veins measured from cored samples generally strike from W to NNW with steep dips (Fig. 3a) and foliations strike NW with shallow west dips (Fig. 3b). From this information, values for p, p' and v were determined for each vein and shear strains were calculated using equation (2) of Skjernaa (1980) (Fig. 4).

The results of strain analyses are presented in Figs. 7–10. Shear strains range from 0.05 to 10.2 and average 2; most veins have values less than 2 (Figs. 7 and 10). Strain magnitudes are not correlative with particular vein generations, which have different undeformed strikes, nor

with particular vein compositions (Fig. 7) which is consistent with the observation that measured veins formed before shearing and behaved as passive markers. Therefore, all veins experienced the same deformational event and can legitimately be used for strain analysis.

A direct relationship exists between the amount of vein rotation (dip change) and shear strain magnitude (Fig. 8a) which is consistent with simple shear deformation as shown in Figs. 5 and 8(b): during a noncoaxial, rotational deformation, vein rotation is a function of shear strain and initial vein orientation. Additionally, veins are deflected gradually and smoothly away from the undeformed shear zone walls through the shear zones which is consistent with strain compatibility requirements. Veins with shallow dips rotate fewer degrees with increasing strain and veins with steeper dips rotate more as documented by Ramsay (1980) and Skjernaa (1980). The scatter away from a single line in Fig. 8(a) results from deformation of veins that have different orientations (Fig. 8b). The spatial distribution of strain within individual shear zones is shown for shear zones on S. Palmaria Island in Fig. 9. Within a shear zone, strain magnitudes generally vary smoothly but show no systematic variation laterally over long distances (Fig. 9b). Additionally, strains vary from zone to zone, showing no systematic variation vertically. These results suggest that the shear zones did not experience progressively higher strains in any direction. There are, however, rare regions where high strains are adjacent to low strains. In most cases there is a local heterogeneity, such as a dolomitized region or an irregular shear zone boundary, that created a local stress concentration which resulted in an anomalously high strain value. In rare cases, there is no obvious rheologic cause for the unusual strain relationship (Fig. 9b; upper right). If these regions represent shear zone terminations they are not accompanied by layer-parallel shortening or extension (see next section) as proposed by Coward (1976).

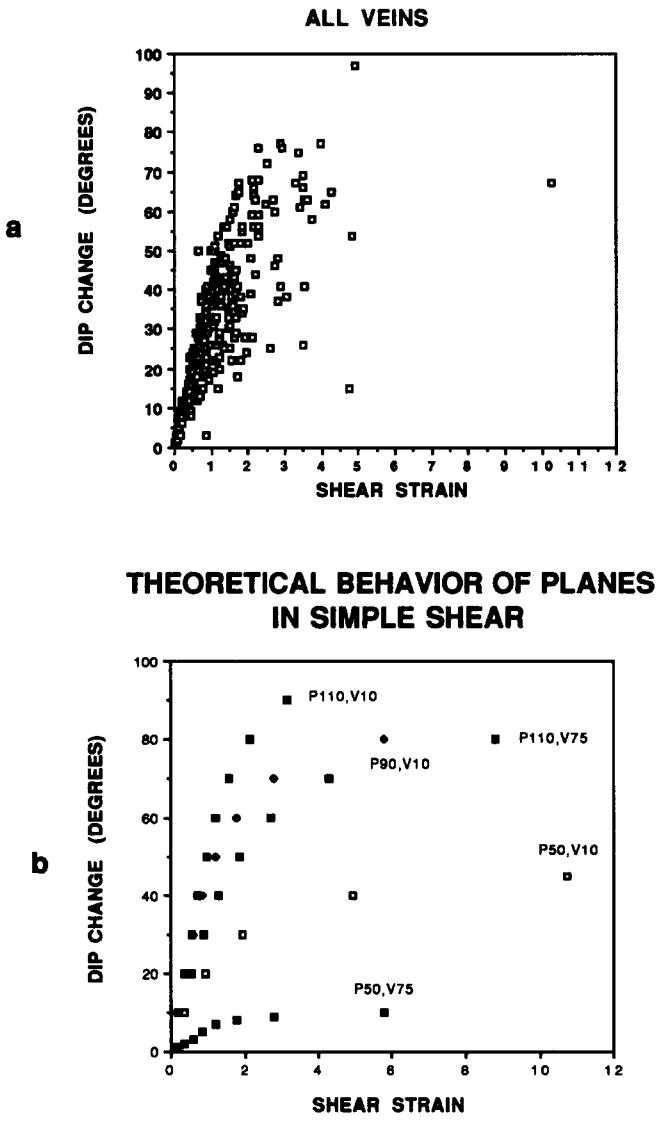

Fig. 8. (a) Dip change ($p - p'$) for measured veins with various angles of v and p vs calculated shear strain (p and p' are the angles between the vein and shear plane in the undeformed and deformed states, respectively). (b) Plot of dip change ($p - p'$) for theoretical veins for various angles of v and p vs resultant shear strain (v is the angle between the vein strike and b-direction). For example, veins with shallow dips that strike at a large angle to b will plot along the lowest line on (b) whereas veins with steep dips that strike at a small angle to b will plot along the steepest line (b).

The average strain and range of strain magnitudes are equivalent within the Portoro from each of the five quarries (Fig. 10). There are, however, packages containing several shear zones that show consistently high or low strains. For example, in the southern quarry (SP), shear strain magnitudes from shear zones within the upper and lower sections are larger than from those within the middle section (Fig. 9b). This is perhaps a function of the proximity of a package of shear zones to the dolomitized contacts of the Portoro, or the amount of dolomitization of undeformed layers bounding each shear zone. The upper and lower shear zone packages are adjacent to dolomitized contacts and undeformed layers within the middle package of shear zones appear less dolomitized than other packages. Shear zones with large strains, therefore, probably reflect stress concentrations resulting from adjacent, massively dolomitized regions and shear zones with small strains reflect weaker stress concentrations from the lack of adjacent competent layers.

The general direction of tectonic transport, a-direction, during shearing was toward the NE as determined from the orientation of the shear-related foliation in shear zones, which strikes perpendicular to a (Ramsay 1967). Shear zones in each quarry show nearly parallel, NE-directed transport ranging from approximately N40E to N65E (Fig. 3b).

Displacement resulting from shearing, as calculated from strain magnitudes and shear zone widths, according to equation (39) from Ramsay & Graham (1970, p. 799), average approximately 15–40 cm per zone. The total displacement for the 80 m-thick stack of shear zones, based on the average shear strains for each layer, is between 49 and 79 m. Total offset is higher, however, because many highly strained zones were not sampled. Strain in those zones was too high to quantify because veins could not be traced into shear zone centers.

Results from strain analyses of veins in shear zones

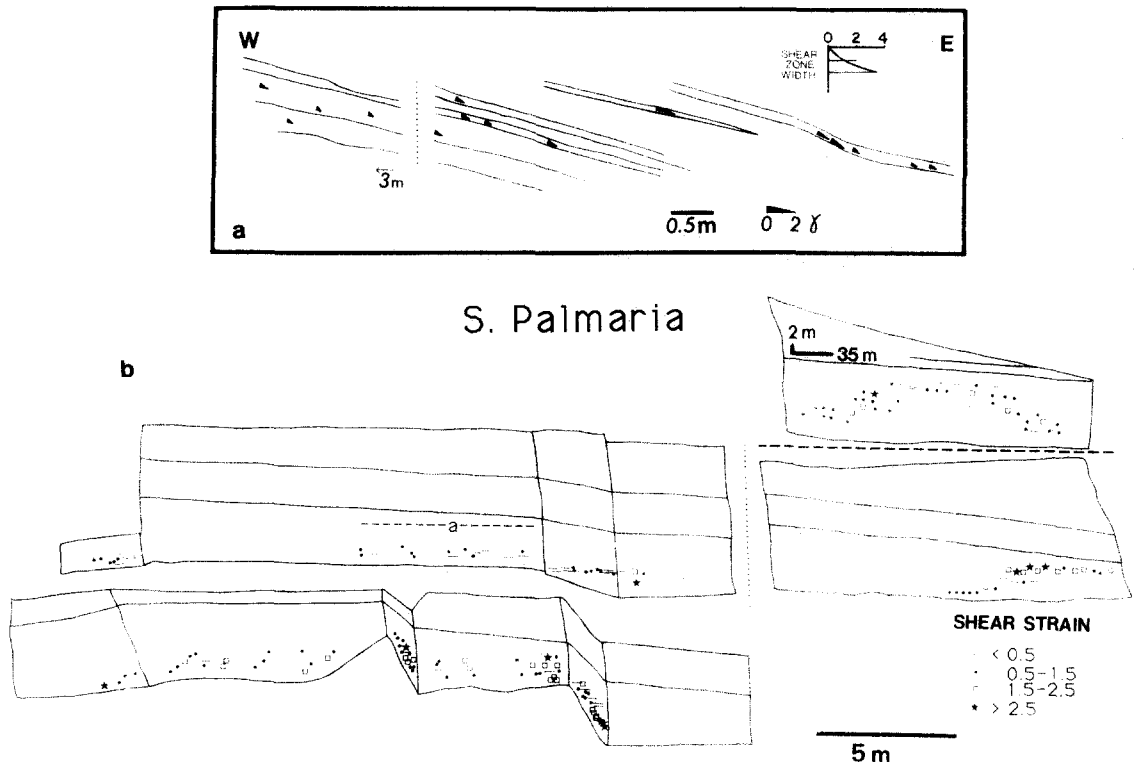

Fig. 9. (a) Sketch of South Palmaria (see Fig. 1) quarry face and strain magnitudes from cored locations. Length of triangle represents shear strain magnitude as illustrated by diagram in inset; x-axis represents shear strain (that of unfilled triangle in inset is approximately 4, that of filled triangle along basal border is approximately 2); y-axis represents shear zone width according to bar scale shown at base. Dotted line represents break in section of approximately 3 m. (b) Three-dimensional sketch of quarry (SP) (see Fig. 2c) showing three levels with locations of cored samples indicated. Relative shear strain magnitudes: stars—high strain (greater than 2.5), square—moderate strains (greater than 1.5, less than 2.5), dot—moderately low strains (greater than 0.5, less than 1.5), dash—low strains (less than 0.5). Dotted line represents break in section of 10 m; dashed line represents break in section of 35 m toward right and 2 m vertically (see arrows in upper left). Note the general consistency in shear strain magnitudes and differences in strain magnitudes between quarry levels. Face shown in (a) is indicated.

(Figs. 7–10) are consistent with a simple shear strain history because the amount of vein rotation in shear zones is a function of the shear strain and the original vein orientation (Fig. 8) as proposed by Skjernaa (1980). The heterogeneous distribution of strain is consistent with deformation that did not progress in any particular direction. The packages of relative large and small strains probably reflect stress concentrations caused by differences in rheology.

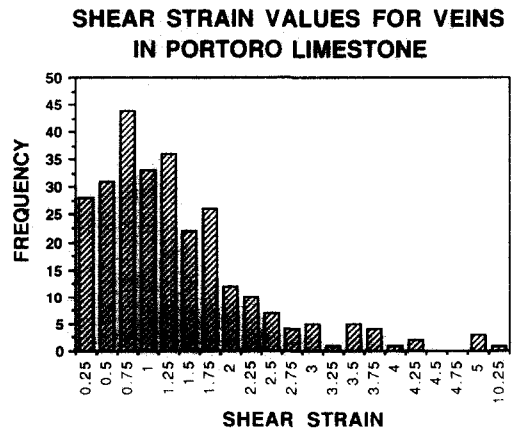

Fig. 10. Shear strain values determined from vein orientations according to equation (1). The number given at each x-axis division represents shear strain values between that number and the previous division. Average shear strain values from each quarry (see Fig. 1) are as follows: MC = 1.3 (eight samples); CQ = 0.7 (23 samples); CT = 1.8 (five samples); NP = 2.0 (46 samples); and SP = 1.1 (194 samples).

Layer-parallel shortening/extension and wrench-type shear. If shear zones experienced additional components of strain, such as wrench-type shear or layer-parallel shortening or extension (hereafter referred to as pure shear), as a result of initiation points similar to those proposed by Coward (1976), the effects should be recorded by a change in the strikes of veins within the shear zones. To check these effects, first the orientations of veins within only undeformed layers were determined for the purpose of documenting the natural variation in the strikes of veins that had not been strained. Second, geometric analysis of veins in undeformed layers and shear zones, combined with Fry (1979) analysis of pellets within sections parallel to the shear plane were completed.

The variability in the orientations of veins that were traced through serial slabs of undeformed layers (Fig. 11a) shows that veins are not strictly planar. The variation in the trend of a vein on planes parallel to the shear (*ab*) plane (strike of the vein if bedding is horizontal), ranges from 0° to more than 20° (Fig. 11a). Veins with strike variations greater than 20° were generally thin, wispy, discontinuous calcite veins (Fig. 11b). This type

of vein was avoided in the strain analyses. The other wider, more continuous veins varied in strike less than 20°. This value will, therefore, represent the upper, acceptable limit of natural strike variation for veins that have not been strained.

The changes in vein strikes from the undeformed layers into the shear zones are not consistent with pure shear or wrench-type shear. A comparison between the strikes of veins in the undeformed layers and in shear zones shows a well-defined linear relationship (Fig. 12a). This relationship is not consistent with layer-parallel shortening or extension which would produce a significant change in the strike of veins within shear zones (Fig. 5b) compared to their undeformed orientation. The resulting trend would show a significant deviation from the line $k = 1$. A component of wrench-type shear would produce a unidirectional rotation of the strikes of veins in shear zones away from the strikes of the undeformed veins (Fig. 5a). This rotation is not present in Fig. 12(a) reflecting the absence of wrench-type shear. Additionally, a comparison between the strike changes of veins between undeformed layers and shear zones with the angle v (Fig. 12b) shows a concentration that is not consistent with pure shear in two ways: (1) layer-parallel shortening along the a-direction would have caused larger strike changes for veins that strike at an angle to the b-direction (Fig. 5b); and (2) vein strikes would have rotated toward the b-direction resulting in small angles of v (Fig. 5b) and a linear trend along $v = 0$ on Fig. 12(b).

Nearly all of the veins, 91%, maintain their strike to within 20° (Fig. 12b) upon passing from undeformed layers into shear zones. The minority of veins, 9%, that show strike changes greater than 20° probably reflect a natural variation in strike during vein formation rather than layer-parallel shortening for the following reasons. If layer-parallel shortening had produced large strike changes, the dips of those veins would have been steeper resulting in smaller dip changes and, therefore, in apparently smaller shear strains. Instead, shear strains associated with veins that show large strike changes are equivalent to those of veins that show no significant strike changes (Fig. 13). Additionally, in most cases, field photographs and careful examination of cores containing veins with large strike changes, revealed local, physical perturbations, such as dolomite buttresses, small irregularities in the shear zone wall, late minor fault movement and vein networks (Fig. 6b). These perturbations would certainly cause local stress concentrations that would affect the orientations of veins during their formation and during deformation and would clearly not represent processes associated with shear zone formation. Thirteen veins, however, showed large strike changes yet showed no obvious local perturbation. Four

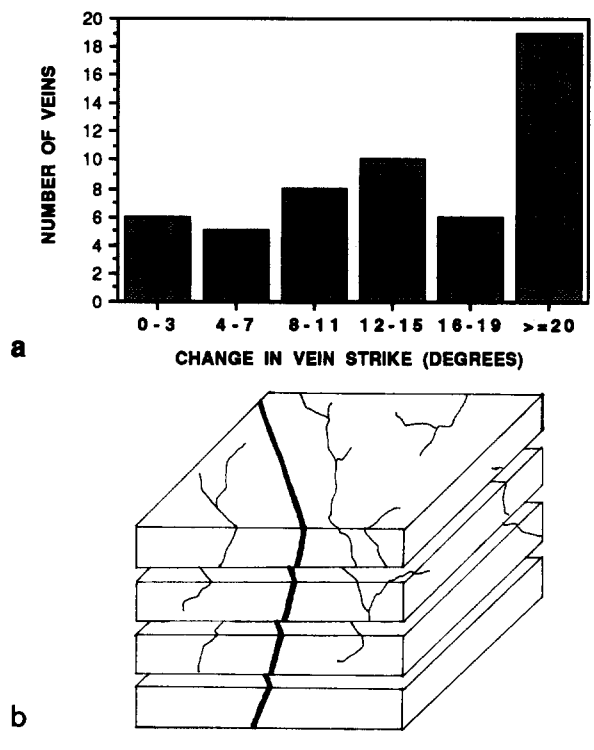

Fig. 11. Natural undeformed vein strike variation. Variation in strikes (trend on shear plane) of individual veins in undeformed layers traced through serial slabs (see b below). Those with strike changes over 20° were generally wispy, thin veins (b) Sketch of undeformed sample sawed into serial slabs parallel to the shear plane so that vein strikes could be traced on the *ab* plane through each slab. The trace of most veins, such as the yellow carbonate–sediment-filled vein (heavy line) is relatively constant whereas the traces of thin, wispy white carbonate veins (thin lines) are variable.

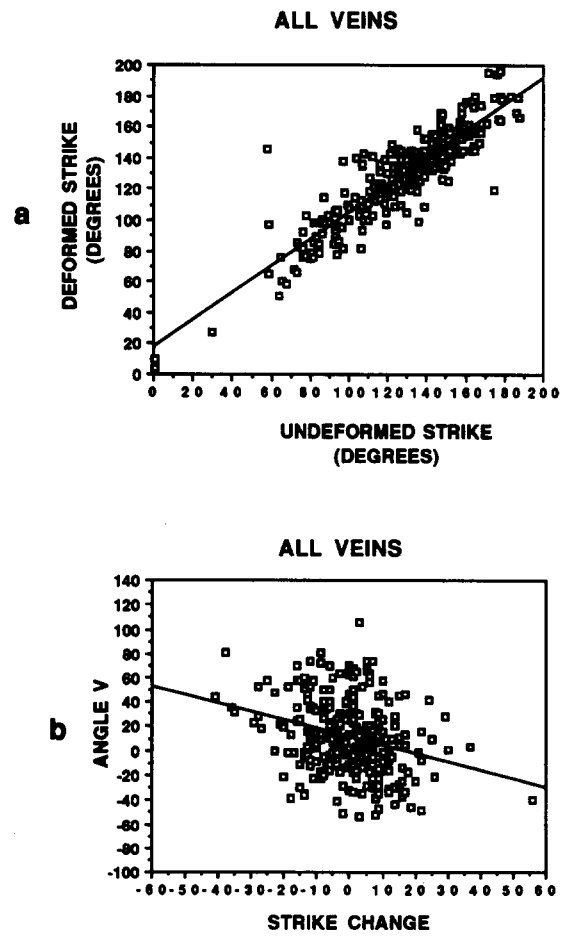

Fig. 12. (a) Strikes of veins in shear zones and in undeformed layers. (b) Change in vein strikes compared to the angle v (angle between vein strike and b-direction). Lines are best fit.

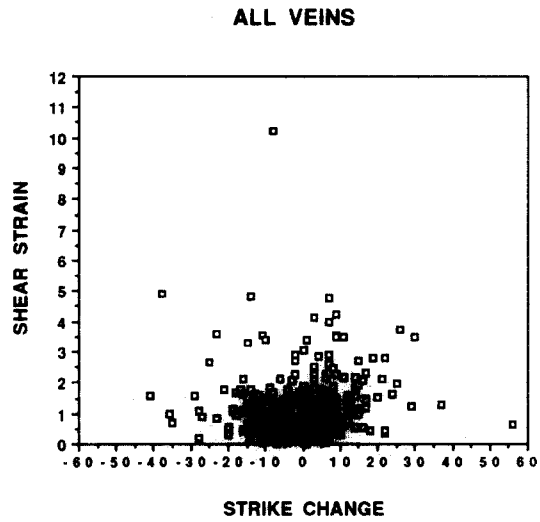

Fig. 13. Change in vein strikes compared to shear strain.

of these samples contained pellets suitable for strain analysis, and Fry (1979) analyses were completed on sections parallel to the shear plane. Fry analysis is a measure of the relative displacement of the centers of randomly distributed, closely packed circular objects. If a rock is undeformed, the central vacancy of the cluster will be circular, indicating equidistant neighbors in all directions. If the rock is deformed, the central vacancy will be an ellipse that records the bulk change in shape of the rock as shown by the packing of objects. These analyses show circular rather than elliptical centers (Fig. 14) indicating no effect of coaxial strain, volume change or strain in the *b*-direction.

In summary, the results presented above show that the shear zones did not experience general pure shear or wrench-type shear components. The large strike changes observed in 9% of the samples probably reflect a natural strike variation during vein formation analogous to those seen in undeformed serial slabs (Fig. 11), or the influence of local strain heterogeneities within shear zones resulting from local, physical perturbations that formed prior to shearing. In either case, there is no evidence to support the existence of a pure shear deformational component that would represent initiation points such as those proposed by Coward (1976).

Volume change. The existence of volume change in general is usually very difficult to document and this is also true for the Portoro shear zones. The Fry analyses discussed above, however, show that at least for those samples, non-uniform volume change did not occur. Another test for volume change would be to determine whether two veins in the same sample show different shear strains. However, because there is never more than one measurable vein in each core, this method cannot be used. Alternatively, if large and small shear strain magnitudes lie adjacent to one another within a shear zone in the absence of other strain components (as documented in the previous section), local volume changes must have occurred. Figures 6(c) & (d) show one of the three points within different shear zones where an anomalously large shear strain (and therefore large displacement) lies adjacent to a small strain (and therefore small displacement). The amount of area loss that occurred at these locations can be determined by calculating the difference in displacement between veins

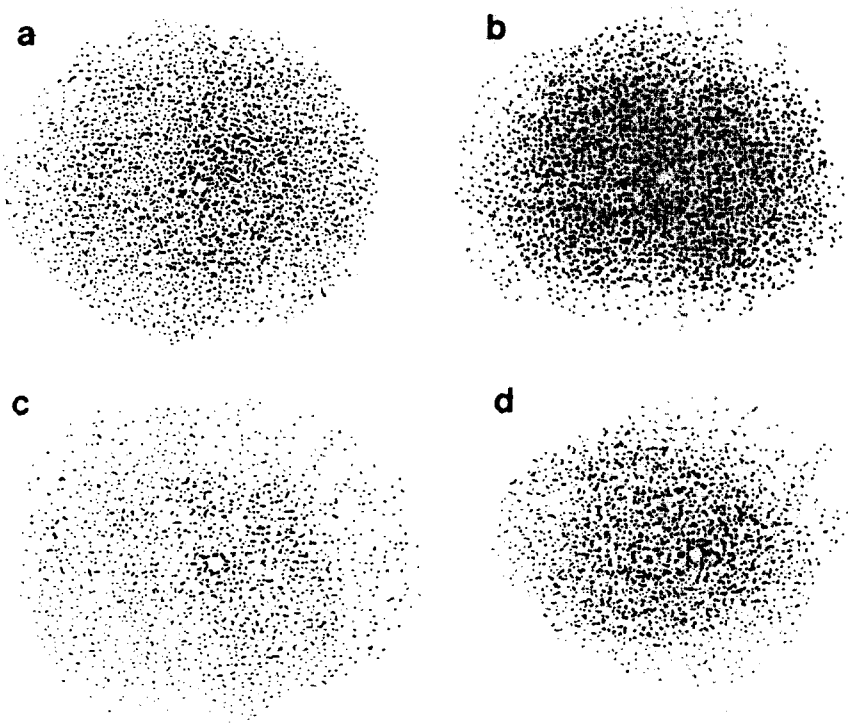

Fig. 14. Plots from Fry (1979) analysis of pellets within shear zones in planes parallel to the shear plane. Analyses are from cores in which a vein showed no strike change from undeformed to shear zone (a), and large strike changes; (b) 56°, (c) 16° and (d) 29°. Note the circular center of each case.

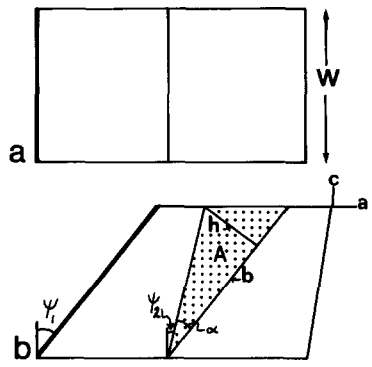

Fig. 15. Calculation of area loss between two veins that show different shear strain magnitudes. (a) Represents a layer in the undeformed state. Heavy lines represent vein traces on the *ac* plane of future shear zone. (b) Represents the layer shown in (a) in the deformed state. The left half of the layer experienced greater shear strain than the right half (vein represented by the heavy line (leftmost) shows higher shear strain than vein represented by thinner line). The shaded triangle represents that area loss, A, between veins. ψ_1 = angular shear of heavy line; ψ_2 = angular shear of thinner line; $A = (bh)/2 = 1/2\{(w \tan \psi_2)^2 + w^2\}^{1/2}\{(w \tan \psi_1)^2 + w^2\}^{1/2} \sin \alpha$; w = shear zone width; $\alpha = 90 - \psi_2$.

as shown in Fig. 15. Area losses for these three locations are 24, 28 and 33% which suggests that some volume loss locally accompanied the non-coaxial, rotational strain. Although these three points must also represent sites of strain incompatibility (see Ramsay & Huber 1983, section 3), the strain gradient is still relatively smooth because of the large distance (equal to or greater than the shear zone width) across which the minor volume loss occurs. The consistency in shear strain laterally over large distances in all the areas, as well as the continuous nature of veins even at a microscopic level, argue against volume loss being an important factor throughout. Volume change in some places should be expected because shear zones also contain evidence of fluid interaction (Carter 1990, Carter & Dworkin 1990) that would facilitate volume change.

MODEL OF SHEAR ZONE FORMATION

Bedding-parallel, ductile shear zones in the Portoro appear to have formed as a result of simple shear strain and local, minor volume loss. Strain is heterogeneously distributed both laterally along shear zones and vertically throughout the stack: however, packages of relatively homogeneous, laterally continuous strains exist. The absence of additional strain components, the relative simplicity of the strain, and the lack of evidence for brittle precursors or plastic instabilities within shear zones suggests that the zones did not form according to previously proposed models (e.g. Coward 1976, Ramsay & Allison 1979, Poirier 1980, Segall & Simpson 1986). Instead, the zones appear to have initiated in layers of easy slip that propagated under conditions of non-coaxial, rotational strain. Shear zones developed within limestone layers that are much less dolomitized than adjacent undeformed layers of mixed limestone and dolomite. The competent layers of mixed dolomite and calcite layers probably caused lateral stress concentrations along the limestone layers, analogous to that formed in putty between moving bricks, resulting in shear zone initiation at the onset of thrusting. There was apparently not a single point of initiation within a zone or within the 80 m stack of zones as reflected by the absence of shortening in any parts of any zone and the lack of systematic variation in shear strains in particular layers. Therefore, at the onset of deformation, the zones might have slipped nearly synchronously like a card deck pushed from behind. The planar nature of the zones (Figs. 2a–c, 6a,c & d and 9) suggests that further development, or propagation, of the zones was easy (e.g. Coward 1976). Propagation during non-coaxial, rotational strain was probably facilitated by the presence of fluids that enhanced dynamic recrystallization of calcite (Carter & Dworkin 1990) resulting in strain softening (Ramsay & Graham 1970, Carter 1990).

CONCLUSIONS AND TECTONIC IMPLICATIONS

The deformation of passive markers within bedding-parallel ductile shear zones in the Portoro Limestone reflects a simple shear, or non-coaxial, rotational strain history, with local minor volume change, in which shear zones probably initiated synchronously and propagated uniformly and easily. Shear stains are generally uniformly distributed along shear zones and show no lateral or vertical systematic variations. The relatively simple strain history is not typical for deformation zones in other tectonic settings at depths of 7–10 km where shear zones are generally wider, show brittle behavior, and experienced more intense coaxial, wrench-type and non-coaxial strains (e.g. Coward & Kim 1981, Kligfield *et al.* 1981, Sanderson 1982). In addition, the relatively simple kinematic history probably reflects bulk, synchronous movement similar to card-deck shear which is unlike most thrust propagation models that show thrusts younging with depth and toward the foreland. These differences are probably the result of rheologic properties of the Portoro and the strain softening influence of syndeformational fluids. Calcite alternating with mixed calcite and dolomite layers provided a natural rheologic situation for strain to be partitioned into calcite layers. The spacing and thickness of these layers are generally uniform throughout the Portoro so that preferential movement did not occur in a particular layer. Syndeformational fluids that enhanced the dynamic recrystallization of calcite caused strain softening that probably resulted in easy propagation of shear zones.

The tectonic implications that can be inferred from the simple strain and kinematic history recorded by these shear zones are that: (1) the shear zones might represent an internally deformed thrust package between over- and underlying thrust faults that propagated relatively easily during Mid-Tertiary NE-directed thrusting; (2) during NE-directed thrusting, ramps probably did not form nearby (e.g. Fischer & Coward 1982). If any ramps did develop in the nappe, however, the

shear zones must have formed and remained behind them (hinterlandward); and (3) the geometry of deformation zones and type of strain produced within them depends strongly on the rheology and structural configuration of the stratigraphic packages involved in the deformation.

Acknowledgements—This work represents part of the author's Ph.D. dissertation. I am grateful to Sharon Mosher and Robert Folk for their generous advice and rigorous reviews of this manuscript. I thank Brian Reck, Win Means and Roy Kligfield for helpful discussions and Iain Allison and Lilian Skjernaa for their insightful and constructive reviews of the manuscript. Assistance from Tom Hoak, the quarry men and the Italian military on Palmaria Island was instrumental to this study. Grants to the author from Sigma Xi, The Geological Society of America, The American Association of Petroleum Geologists, and the Geology Foundation of the University of Texas at Austin are very gratefully acknowledged as is funding from NSF grant EAR-8721302 to S. Mosher.

REFERENCES

Berthé, D., Choukroune, P. & Jegouzo, P. 1979. Orthogneiss, mylonite and non-coaxial deformation of granites: the example of the South Armorican shear zone. *J. Struct. Geol.* **1**, 31–42.

Boullier, A. M. 1986. Sense of shear and displacement estimates in the Abeibara-Rarhous late Pan-African shear zone, Adrar des Iforas, Mali. *J. Struct. Geol.* **8**, 47–58.

Burg, J.-P. & Laurent, Ph. 1978. Strain analysis of a shear zone in a granodiorite. *Tectonophysics* **47**, 15–42.

Capellini, G. 1862. Studi stratigrafici e paleontologici sull'Infralias del Golfo della Spezia. *Mem. Acc. Sci. Bologna* **2**, 247–318.

Carmignani, L., Gaetano, G. & Kligfield, R. 1978. Structural evolution of the Apuane Alps: an example of continental margin deformation in the Northern Apennines, Italy. *J. Geol.* **86**, 487–504.

Carter, K. E. 1990. Construction and collapse of an orogen: Tectonic, strain and fluid history of the Tuscan nappe, Northern Apennines, Italy. Unpublished Ph.D. dissertation, University of Texas at Austin.

Carter, K. E. & Dworkin, S. I. 1990. Channelized fluid flow through shear zones during fluid-assisted dynamic recrystallization, Northern Apennines, Italy. *Geology* **15**, 720–723.

Carter, K. E. & Mosher, S. 1987. Apennine thrusting and post-Apennine gravity sliding in the Portovenere area, N. Apennines, Italy. *Geol. Soc. Am. Abs. w. Prog.* **19**, 613.

Carter, K. E., Mosher, S. & Folk, R. 1991. Construction and collapse recorded in the Tuscan nappe, La Spezia area, N. Apennines, Italy. In: *Geologia del Basamento Italiano* (edited by Lazzarotto, A. *et al.*). Università di Siena, 134.

Ciarapica, G., Passeri, L. & Stoppa, F. 1985. Convegno "G. Capellini", Guida all'escursione, La Spezia, Università di Perugia.

Coward, M. P. 1976. Strain within ductile shear zones. *Tectonophysics* **34**, 181–197.

Coward, M. P. & Kim, J. H. 1981. Strain within thrust sheets. In: *Thrust and Nappe Tectonics* (edited by McClay, K. R. & Price, N. J.). *Spec. Publs geol. Soc. Lond.* **9**, 275–292.

Davis, G. A., Lister, G. S. & Reynolds, S. J. 1986. Structural evolution of the Whipple and South Mountains shear zones, southwestern United States. *Geology* **14**, 7–10.

Fazzuoli, M. 1980. Frammentazione ed "annegamento" della piattaforma carbonatica del calcare massiccio (Lias inferiore) nell'area Toscana. *Mem. Soc. geol. Ital.* **21**, 181–191.

Fischer, M. W. & Coward, M. P. 1982. Strain and folds within thrust sheets: an analysis of the Heilam Sheet, northwest Scotland. *Tectonophysics* **88**, 291–312.

Folk, R. L. 1988. Discovery in Columbus' land: Carbonate mud diagenesis to microspar or metamicrite? *Soc. econ. Paleont. Miner. Abs.* **5**, 19.

Folk, R. L., Pursell, V. J., Greenberg, J., Mosher, S., Helper, M. & Carter, K. E. 1989. Inverted tectonic veins in the Triassic Portoro Limestone, Portovenere area (La Spezia), Italy. *Annales Tectonicae* **3**, 25–33.

Fry, N. 1979. Random point distributions and strain measurement in rocks. *Tectonophysics* **60**, 89–105.

Gapais, D., Bale, P., Choukroune, P., Cobbold, P. R., Mahjoub, Y. & Marquer, D. 1987. Bulk kinematics from shear zone patterns: some field examples. *J. Struct. Geol.* **9**, 635–646.

Ghosh, S. K. & Sengupta, S. 1987. Progressive development of structures in a ductile shear zone. *J. Struct. Geol.* **9**, 277–287.

Kligfield, R., Carmignani, L. & Owens, W. H. 1981. Strain analysis of a Northern Apennines shear zone using deformed marble breccias. *J. Struct. Geol.* **3**, 421–436.

Miller, J. 1988. Multistage dolomitization of the Portoro Limestone, Liguria, Italy. Unpublished M.A. thesis, University of Texas at Austin.

Poirier, J. P. 1980. Shear localization and shear instability in materials in the ductile field. *J. Struct. Geol.* **2**, 135–142.

Ponce de Leon, M. I. & Choukroune, P. 1980. Shear zones in the Iberian Arc. *J. Struct. Geol.* **2**, 63–68.

Ramsay, J. G. 1967. *Folding and Fracturing of Rocks.* McGraw-Hill, New York.

Ramsay, J. G. 1980. Shear zone geometry: a review. *J. Struct. Geol.* **2**, 83–99.

Ramsay, J. G. & Allison, I. 1979. Structural analysis of shear zones in an alpinized Hercynian granite. *Schweiz. miner. petrogr. Mitt.* **59**, 251–279.

Ramsay, J. G. & Graham, R. H. 1970. Strain variations in shear belts. *Can. J. Earth Sci.* **7**, 786–813.

Ramsay, J. G. & Huber, M. I. 1983. *The Techniques of Modern Structural Geology, Volume 1: Strain Analysis.* Academic Press, London.

Sanderson, D. J. 1982. Models of strain variation in nappes and thrust sheets: a review. *Tectonophysics* **88**, 201–233.

Segall, P. & Simpson, C. 1986. Nucleation of ductile shear zones on dilatant fractures. *Geology* **14**, 56–59.

Skjernaa, L. 1980. Rotation and deformation of randomly oriented planar and linear structures in progressive simple shear. *J. Struct. Geol.* **2**, 101–109.

Zaccagna, D. 1936. La geologia del Golfo della Spezia. *Mem. Acc. Lunigianese Sci.* **14**.